Determinant quantum Monte Carlo study of d-wave pairing in the plaquette Hubbard hamiltonian

T. Ying, R. Mondaini, X. D. Sun, T. Paiva, R. M. Fye, and R. T. Scalettar

Phys. Rev. B **90**, 075121 — Published 13 August 2014

DOI: 10.1103/PhysRevB.90.075121

Determinant Quantum Monte Carlo Study of d-wave pairing in the Plaquette Hubbard Hamiltonian

T. Ying[1], R. Mondaini[2,3], X.D. Sun[1], T. Paiva[4], R.M. Fye[5] and R.T. Scalettar[3]
[1] *Department of Physics, Harbin Institute of Technology, Harbin 150001, China*
[2] *Physics Department, The Pennsylvania State University, 104 Davey Laboratory, University Park, Pennsylvania 16802, USA*
[3] *Physics Department, University of California, Davis, California 95616, USA*
[4] *Instituto de Fisica, Universidade Federal do Rio de Janeiro Cx.P. 68.528, 21941-972 Rio de Janeiro RJ, Brazil and*
[5] *Sandia National Laboratories, New Mexico, P.O. Box 5800 Albuquerque, NM 87185*

Determinant Quantum Monte Carlo (DQMC) is used to determine the pairing and magnetic response for a Hubbard model built up from four-site clusters - a two-dimensional square lattice consisting of elemental 2 × 2 plaquettes with hopping t and on-site repulsion U coupled by an inter-plaquette hopping $t' \leq t$. Superconductivity in this geometry has previously been studied by a variety of analytic and numeric methods, with differing conclusions concerning whether the pairing correlations and transition temperature are raised near half-filling by the inhomogeneous hopping or not. For $U/t = 4$, DQMC indicates an optimal $t'/t \approx 0.4$ at which the pairing vertex is most attractive. The optimal t'/t increases with U/t. We then contrast our results for this plaquette model with a Hamiltonian which instead involves a regular pattern of site energies whose large site energy limit is the three band CuO_2 model, and show that there the inhomogeneity rapidly, and monotonically, suppresses pairing.

PACS numbers: 71.10.Fd, 02.70.Uu

I. INTRODUCTION

One of the earliest numerical indications of the possibility that an on-site electron-electron interaction U might play a role in novel superconducting materials was the observation of a negative "binding energy" in exact diagonalization studies of the Hubbard Hamiltonian on 2 × 2 clusters. In this geometry, the ground state energy of two holes doped together into a half-filled system was shown to be lower than if the two holes were on separate clusters:

$$\Delta_p = E_0(2) + E_0(0) - 2\,E_0(1) < 0 \qquad (1)$$

Here $E_0(n)$ is the ground state energy of n holes. The observation that the $n = 2$ and $n = 0$ ground states have s- and d-wave symmetry, respectively, and hence are connected by a d-wave pair creation operator, suggested possible relevance of models involving such 2 × 2 clusters with cuprate superconductors.[1] Pair binding was also studied on larger Hubbard clusters,[2,3] and on other geometries, e.g., on one dimensional chains of varying length,[4] with three electronic bands,[5–7] models with intersite interactions,[8] and the strong coupling t-J limit.[2,9–11]

Following these small cluster studies, a considerable amount of analytic and numeric attention has been focused on the "plaquette Hubbard model" which consists of a periodic array of 2 × 2 plaquettes with hopping t and repulsion U connected by a weaker hybridization t'. It was suggested that the plaquettes act as centers of attraction, which then drive superconductivity in the extended lattice. This picture provides a 'local' counterpart to theories of pairing which focus qualitatively on the exchange of magnetic fluctuations. Perhaps unsurprisingly, the presence of inhomogeneous hoppings introduces new phases to the Mott insulator, antiferromagnetic, and d-wave superconductor typically discussed in the uniform $t = t'$ case. Specifically, the quantum numbers and symmetries of the 2 × 2 plaquette can evolve into a wide variety of ground states when t' is made nonzero.[12] An additional diagonal hopping can also change the ground state of the 2 × 2 plaquette building block[13] and induce new types of crystalline insulators. The effects of both chemical potential and hopping disorder on pair binding have been examined,[14] and were shown to be less damaging to superconductivity when there is a plaquette structure compared to the uniform case.

A key conceptual question concerns the existence of an 'optimal inhomogeneity'.[15–17] As pointed out by Tsai and Kivelson,[18] pairing which exists at very weak t' is expected to exhibit a critical temperature T_c which increases as t' grows. If it were the case that T_c is small or zero in the homogeneous model $t' = t$, this necessarily implies a maximal T_c at an intermediate value $0 < t'/t < 1$. Early work relevant to this issue looked at pair binding energies when two plaquettes were linked in different geometries[19]. For the cubic (fully connected) configuration, a maximum binding was found for $t'/t \approx 0.3$ at $U/t = 4$ and for $t'/t \approx 0.5$ when $U/t = 8$. Exact diagonalization of 4 × 4 clusters[20] indicated that the overall maximum occurs at $t'/t \approx 0.5$ and $U/t \approx 8$. Additional evidence for an optimal inhomogeneity in the plaquette Hubbard model is provided by a contractor-renormalization (CORE) study[21] where the pair binding energy was found to be maximized in the range $0.5 < t'/t < 0.7$ and $5 < U/t < 8$.

In related work, the density matrix renormalization

group method has been used to study a collection of 2 × 2 plaquettes connected to form a two leg ladder.[22] It was found that, close to half-filling, $U/t \approx 6$ and $t'/t \approx 0.6$ gives the optimal pair binding energy. Although there can be no finite temperature transition in such one-dimensional ladder geometries, an interchain mean field theory suggests that the critical temperature again exhibits an 'optimal degree of inhomogeneity' with a maximum occurring at $t' < t$.

There have also been several methods which challenge the idea of an optimal inhomogeneity at intermediate t'/t. The central result of a Dynamical Cluster Approximation (DCA) analysis[23] was that the critical temperature T_c for d-wave pairing is maximal for $t'/t = 1$ for interaction strengths U of the order of the bandwidth and lattice fillings $\rho \approx 0.9$. That is, inhomogeneity monotonically suppresses superconductivity. The qualitative physical picture behind this conclusion was that inhomogeneities reduce the magnetic contributions to the pairing interaction.[24–26]

Cellular Dynamical Mean Field Theory (CDMFT) is another approach with which the plaquette Hubbard Hamiltonian has been analyzed.[27] At weak coupling, inhomogeneity reduces the order parameter for small to intermediate doping, but enhances it at larger doping. For strong coupling, inhomogeneity suppresses pairing for all doping. Overall, the CDMFT results seem generally consistent with those of the DCA, namely that for inhomogeneity in the nearest-neighbor hopping such as is present in the plaquette Hubbard model, the superconducting order parameter does not exceed that of the uniform system.

The contrasting results between the DMRG interchain MFT, CORE, and exact diagonalization treatments, and other cases in which optimal inhomogeneity occurs, on one hand, and the DCA, CDMFT methods on the other, provide the motivation for the work described in this manuscript - a study of the plaquette Hubbard Hamiltonian[28] using the Determinant Quantum Monte Carlo method.[29,30] After presenting our new results, we will discuss some of the possible origins of the range of conclusions concerning the underlying physics of this model.

The remainder of this paper is organized as follows: In Sec. II we write down the plaquette Hubbard Hamiltonian and discuss the measurements we use to monitor d-wave pairing. We also provide a brief summary of the DQMC algorithm and its limitations. In Sec. III we discuss our results at half-filling and in the doped case. Our central conclusion is that an optimal degree of inhomogeneity does occur in the plaquette Hubbard model, although the largest pairing signal appears to occur at $t'/t \approx 0.4$ for $U/t = 4$, a bit less than that reported in other work. This optimal t'/t increases with U/t at half-filling. The sign problem restricts us to higher temperatures than those accessible in the DCA[23] and CDMFT[27] approaches. Section IV discusses the effect on pairing of another form of inhomogeneity in which the site energies are varied periodically across the lattice, and Sec. V concerns the sign problem. The paper concludes with a summary of our findings.

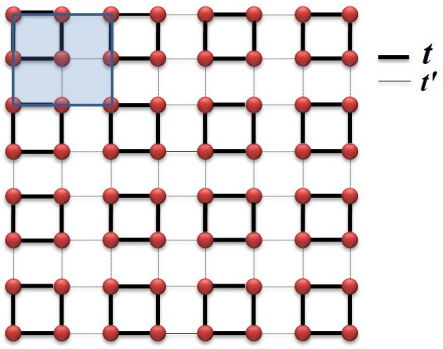

FIG. 1: (Color online) Lattice geometry for the plaquette Hubbard model, a 2D square lattice built from plaquettes of strong hopping t connected by weaker hopping t'.

II. THE PLAQUETTE HUBBARD HAMILTONIAN

The plaquette Hubbard Hamiltonian is

$$\begin{aligned}\hat{H} = &- t \sum_{\langle ij\rangle \in \mathcal{P},\sigma} \left(c^\dagger_{i\sigma} c_{j\sigma} + c^\dagger_{j\sigma} c_{i\sigma} \right) \\ &- t' \sum_{\langle ij\rangle \notin \mathcal{P},\sigma} \left(c^\dagger_{i\sigma} c_{j\sigma} + c^\dagger_{j\sigma} c_{i\sigma} \right) \\ &+ U \sum_i \left(n_{i\uparrow} - \frac{1}{2} \right) \left(n_{i\downarrow} - \frac{1}{2} \right) - \mu \sum_i (n_{i\uparrow} + n_{i\downarrow})\end{aligned} \tag{2}$$

Here $c^\dagger_{i\sigma}\,(c_{i\sigma})$ are the usual creation(destruction) operators for fermions of spin σ on lattice site i. The designations $\langle ij\rangle \in \mathcal{P}$ and $\langle ij\rangle \notin \mathcal{P}$ in the kinetic energy terms convey the fact that hopping t between near neighbor sites i, j on the same plaquette is different from the hopping t' for sites i, j on different plaquettes. This geometry is illustrated in Fig. 1. We have written the interaction term in particle-hole symmetric form, so that $\mu = 0$ corresponds to half-filling. (Note that the Hubbard Hamiltonian with near-neighbor hopping on a bipartite lattice is particle-hole symmetric for *any* pattern of intersite hoppings t_{ij}, and hence, in particular, for the case considered here.)

Although we have referred to t' as the 'interplaquette hopping', so that $t' = 0$ is the limit of independent 2 × 2 clusters, we note that setting $t = 0$ also results in a collection of decoupled 2 × 2 t' clusters. More generally, the Hamiltonian is invariant[23,27] under the interchange of t and t'. As a consequence, there is no need to explore the physics of $t'/t > 1$. The Hamiltonian is also invariant when the values of t and t' are interchanged only on the horizontal links, or only on the vertical links. Our numerical approach preserves all these symmetries.

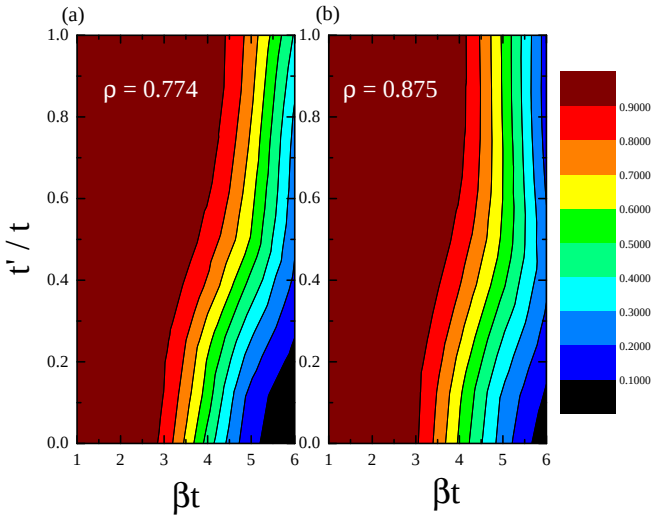

FIG. 2: (Color online) The average sign $\langle \mathcal{S} \rangle$ is shown for the plaquette Hubbard model at $U/t = 4$ and an 8×8 lattice for two different densities. (Because of particle-hole symmetry $\langle \mathcal{S} \rangle = 1$ at $\rho = 1$.) The sign problem becomes somewhat worse with inhomogeneity $t' \neq t$. Roughly speaking, it becomes difficult to generate accurate data in DQMC when $\langle \mathcal{S} \rangle \lesssim 0.3$.

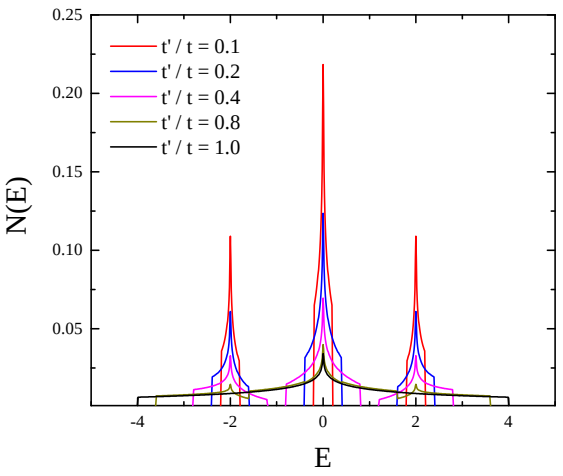

FIG. 3: (Color online) The noninteracting density of states of the uniform ($t' = t$) 2D Hubbard model extends from $-4t$ to $+4t$ and has a van Hove singularity at $E = 0$. In the other limit $t'/t = 0$ there are four discrete (delta function) levels at $E = -2t, 0, 0, +2t$. The density of states is shown here for interpolating ratios of t'/t, exhibiting the evolution between these cases. Regardless of the relative values, Eq. 2 is particle hole symmetric, implying $N(E) = N(-E)$.

In the Determinant Quantum Monte Carlo (DQMC) algorithm[29,30], the expectation values of observables $\langle \hat{A} \rangle = \mathrm{Tr}\, \hat{A} \exp(-\beta \hat{H}) \,/\, \mathrm{Tr} \exp(-\beta \hat{H})$ for fermonic Hamiltonians like Eq. 2 are evaluated by discretizing the inverse temperature β and rewriting the partition function as a path integral. Replacing the exponential of the interaction terms in the Hamiltonian by a coupling of quadratic fermion operators to a Hubbard-Stratonovich field allows the fermions to be integrated out analytically, leaving a product of fermion determinants (one determinant for each spin species) as the weight to sample the Hubbard-Stratonovich field. Each operator $\hat{A}$ can then be measured by accumulating appropriate combinations of Green's functions, the inverse of the matrices whose determinants form the Boltzmann weight. As described further below, the flexibility to alter the order in which the Monte Carlo average is performed and in which the Green's functions are multiplied can be used to control which many body effects are included in the expectation value, and hence to isolate the pairing vertex.

The discretization of β introduces a 'Trotter error'. We have used $\Delta\tau = 1/8$ in the work reported here[30,31]. In practice, unless one examines a local quantity like the energy or double occupancy which can be obtained to very high accuracy, the systematic Trotter errors with this choice of $\Delta\tau$ are less than the statistical errors in the measurements we present.

The central limitation to the DQMC algorithm is the sign problem[38] which arises when the product of determinants becomes negative. This will restrict the temperatures accessible in the study reported here, and, as a consequence, temper our ability to make conclusive statements about the effect of inhomogeneity in the case when the system is doped. At half-filling, because spatial variations in the hopping do not destroy particle-hole symmetry, there is no sign problem and DQMC can better access the ground state for any t'/t. Off half-filling data for the average sign $\langle \mathcal{S} \rangle$ are given in Fig. 2. $\langle \mathcal{S} \rangle$ is relatively weakly dependent on t'/t. The lowest accessible temperature is around $T/t \sim 1/5$ for the entire range $0 < t'/t < 1$, although simulations become somewhat more difficult as t'/t decreases. It is possible to get accurate data for certain quantities, like the density, for quite small values of $\langle \mathcal{S} \rangle$. However for more complex quantities like magnetic and pair correlations at large distances, if reasonable accuracy (statistical error bars less than 10%) is desired, then $\langle \mathcal{S} \rangle \gtrsim 0.3$ is needed. $\langle \mathcal{S} \rangle$ is roughly the same for the two densities $\rho = 0.875$ and $\rho = 0.774$ shown. For $\rho = 0.500$, however, $\langle \mathcal{S} \rangle$ is better behaved (not shown) and reliable averages can be obtained for temperatures as low as $T/t = 1/16$, for several values of t'/t.

The spectrum of the $U = 0$ hopping Hamiltonian for an isolated 2×2 plaquette consists of four energy levels, $E = -2t, 0, 0, 2t$. As t' is turned on, these discrete levels broaden until they finally merge into the 2D square lattice density of states $N(E)$ at $t' = t$. This evolution is shown in Fig. 3. At half-filling, where $E_{\mathrm{Fermi}} = 0$, and for small dopings, $N(E_{\mathrm{Fermi}})$ is enhanced by inhomogeneity. In principle this might

lead to a greater tendency to ordered phases, including superconducting ones, although the possibly competing effect of inhomogeneity on the interaction vertex must also be considered.[23]

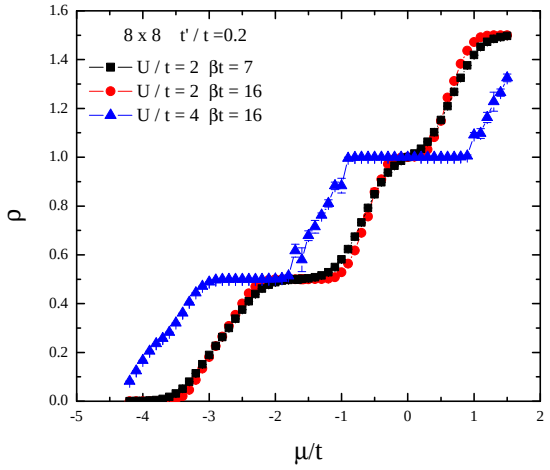

FIG. 4: (Color online) Density as a function of chemical potential for an 8×8 lattice at $t'/t = 0.2$. The band gaps evident in the $U/t = 0$ density of states at $\rho = 0.5$ and $\rho = 1.5$ (Fig. 3) persist at weak to intermediate coupling U/t = 2-4 shown here. (Since ρ is particle-hole symmetric we focus on $\rho \lesssim 1$.) However the interactions also drive the formation of an insulating gap at $\rho = 1$.

For large inhomogeneity ($t'/t < 0.5$) the discrete 2 $\times$ 2 eigen-levels are not sufficiently broadened by t' to coalesce into a single band, and the noninteracting system is a band insulator at $\rho = 0.5$ and $\rho = 1.5$. Figure 4 shows QMC data for $\rho(\mu)$ at interaction strengths $U/t = 2$ and $U/t = 4$ and weakly coupled plaquettes $t'/t = 0.2$. There is a band gap evident at $\rho = 0.5$ (and also, due to particle-hole symmetry at $\rho = 1.5$, not shown). Non-zero U/t is also seen to cause an insulating gap to develop at half-filling, $\rho = 1$. This is a dramatic change from the noninteracting limit, since it represents the suppression of the large peak in $N(E)$ at $E = 0$ in Fig. 3. The development of this gap, even though U/t is much less than the bandwidth, is associated with the onset of long range antiferromagnetic order, as we shall see in the next section. Notice that reasonable data can be obtained for the density even at $U/t = 4, \beta t = 16$. This, however, is not true for more complicated spin and pair correlations.

The equal time spin correlation function and magnetic structure factor are given by,

$$\begin{aligned} c_{\rm spin}(\vec{r}) &= \langle\, m_{\vec{r}_0+\vec{r}}\, m^\dagger_{\vec{r}_0}\,\rangle \qquad m^\dagger_r = c^\dagger_{\vec{r}\uparrow} c_{\vec{r}\downarrow} \\ S^{+-}(q_x, q_y) &= \frac{1}{N}\sum_{i,j} c_{\rm spin}(\vec{r})\; e^{i\vec{q}\cdot\vec{r}} \end{aligned} \tag{3}$$

with an analogous expression for $S^{zz}(q_x, q_y)$. In the

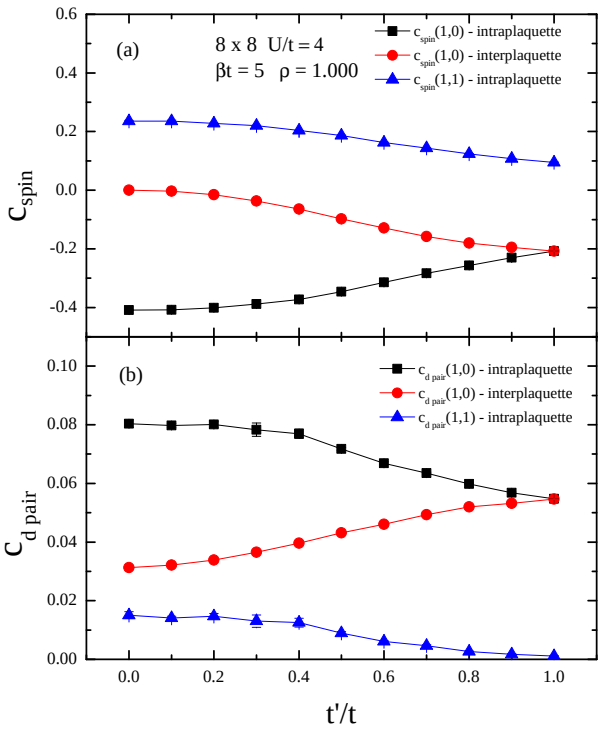

FIG. 5: (Color online) Spin (a) and charge (b) correlations along an intraplaquette bond (black squares), interplaquette bond (red circles), and along the diagonal of the plaquette (blue triangles). Here $\rho = 1$, $U/t = 4$, and $\beta t = 5$. The lattice is 8×8.

homogeneous system it is known that at $T/t = 0$ and at half-filling the 2D Hubbard Hamiltonian possesses long range magnetic order.[30,31,39,40] That is, the spin-spin correlations $c_{\rm spin}(\vec{r})$ in real space approach a nonzero value asymptotically as $|\vec{r}| \to \infty$. On finite sized lattices, this is established by an appropriate scaling of the structure factor with lattice size.[41]

As with magnetic order, a tendency to d-wave pairing can be examined via the asymptotic behavior of equal time correlations,

$$\begin{aligned} c_{d\,\rm pair}(\vec{r}) &= \langle \Delta_{d\,\vec{r}_0+\vec{r}}\, \Delta^\dagger_{d\,\vec{r}_0}\rangle \\ \Delta^\dagger_{d\,\vec{r}} &= c^\dagger_{\vec{r}\uparrow}(c^\dagger_{\vec{r}+\hat{x}\downarrow} - c^\dagger_{\vec{r}+\hat{y}\downarrow} + c^\dagger_{\vec{r}-\hat{x}\downarrow} - c^\dagger_{\vec{r}-\hat{y}\downarrow}) \end{aligned} \tag{4}$$

However, a more sensitive measurement, and one which makes better contact with previous DCA work,[23] is the d-wave pairing susceptibility,

$$\begin{aligned} c_{d\,\rm pair}(\vec{r},\tau) &= \langle \Delta_{d\,\vec{r}_0+\vec{r}}(\tau)\Delta^\dagger_{d\,\vec{r}_0}(0)\rangle \\ \Delta^\dagger_{d\,\vec{r}}(\tau) &= e^{\tau H}\Delta^\dagger_{d\,\vec{r}}(0)e^{-\tau H} \\ P_d &= \sum_{\vec{r}}\int_0^\beta c_{d\,\rm pair}(\vec{r},\tau)\; d\tau \end{aligned} \tag{5}$$

P_d is a preferred diagnostic of superconductivity,

especially if the sign problem precludes going to low temperatures, because it allows for a comparison between the fully dressed susceptibility and the uncorrelated susceptibility $\overline{P}_d$, and hence an indication of pairing even when only short range order is present.[42] The technical distinction between P_d and $\overline{P}_d$ in a DQMC simulation is that when the expectation value of the four fermion terms in Eq. 5 is evaluated, the Green's functions obtained by the Wick contractions are first multiplied together and then averaged to obtain P_d, whereas for $\overline{P}_d$, the Green's functions are first averaged and then multiplied. In $\overline{P}_d$ the effect of the interactions is only to dress the individual single particle propagators, while P_d includes all interaction effects[42].

This distinction allows us to extract the interaction vertex Γ_d from P_d and $\overline{P}_d$:

$$\Gamma_d = \frac{1}{P_d} - \frac{1}{\overline{P}_d} \ . \tag{6}$$

If $\Gamma_d \overline{P}_d < 0$, the associated pairing interaction is attractive. More precisely, Eq. 6 can be re-written as,

$$P_d = \frac{\overline{P}_d}{1 + \Gamma_d \overline{P}_d} \tag{7}$$

so that $\Gamma_d \overline{P}_d \to -1$ signals a superconducting instability.

III. RESULTS

A. Half-Filling

Our central interest is in the doped lattice, where antiferromagnetism might potentially give way to d-wave pairing. However, we begin by briefly showing results at $\rho = 1$, which, as we shall see, are not qualitatively so dissimilar to $\rho < 1$.

Due to the spatial inhomogeneity, spin and pair correlations are not the same on all pairs of near-neighbor (NN) links. In Fig. 5 (a) we show the NN spin correlations $c_{\rm spin}(1,0)$ along an intraplaquette (t) bond and along an interplaquette (t') bond. We also show the next-near neighbor (NNN) correlation $c_{\rm spin}(1,1)$ across the internal diagonal of a plaquette. The NN values are negative, indicating (short-range) antiferromagnetic order. As expected, the interplaquette value vanishes at $t'/t = 0$ and the two NN correlations become degenerate when $t'/t = 1$. The NNN correlations are positive, in agreement with antiferromagnetic behavior.

Figure 5(b) shows the analogous short-range d-wave pair correlations $c_{d\,\rm pair}(1,0)$ and $c_{d\,\rm pair}(1,1)$. The value of $c_{d\,\rm pair}(1,0)$ along an interplaquette (t') bond does not vanish at $t'/t = 0$ owing to the finite spatial size of the d-wave operator (Eq. 5). Short-ranged pairing correlations change very smoothly with t'/t. We will therefore turn to the more sensitive magnetic and pairing structure factors and susceptibilities.

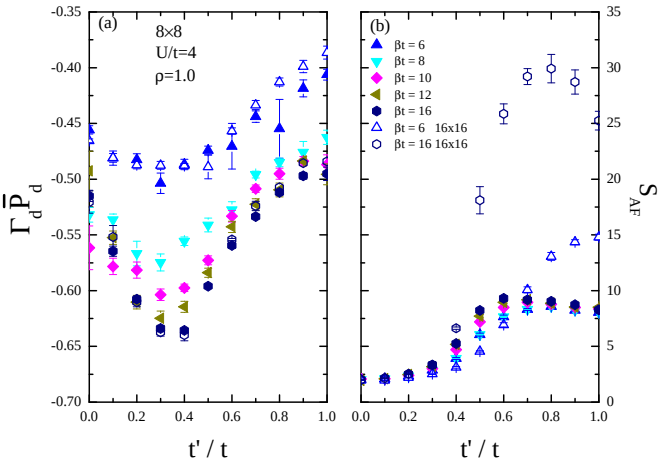

FIG. 6: (Color online) (a) Product of d-wave superconducting vertex Γ and no-vertex pairing susceptibility $\overline{P}_d$ as a function of inter-plaquette hopping t'. Parameters are half-filling ($\mu/t = 0$) and $U/t = 4$. If $\Gamma\overline{P}_d \to -1$, a superconducting instability ensues. Pairing tendency is optimized at intermediate $t'/t \approx 0.40$, and increases as temperature is lowered. Finite size effects (8×8 and 16×16 lattices are compared) are minimal. (b) Antiferromagnetic structure factor $S_{\rm af}$. Long range correlations (antiferromagnetic correlation length exceeds finite size of lattice) does not develop at $\beta t = 16$ until $t'/t \gtrsim 0.6$.

The left panel of Fig. 6 shows the product $\Gamma\overline{P}_d$ of the pairing vertex and the uncorrelated susceptibility. $\Gamma\overline{P}_d$ becomes closest to -1, where a superconducting instability would occur, at an intermediate value $t'/t \sim 0.4$. The tendency to pairing becomes greater as βt is increased (lower temperature). Finite size effects are small, with data for 8×8 and 16×16 lattices largely coinciding.

Fig. 6 (b) shows the antiferromagnetic structure factor $S_{\rm AF} \equiv S(\pi,\pi)$. We emphasize that $\rho = 1$ is privileged from the point of the view of the DQMC algorithm, since there is no sign problem and hence very low temperatures can be simulated. The large values of $S_{\rm AF}$ evident in Fig. 6(b) arise from the development of longer ranged correlations at the low temperatures accessible at $\rho = 1$, so that the spatial sum in Eq. 3 receives contributions from all lattice separations. In principle, $S_{\rm AF} \propto L^2$, the lattice volume, but there are significant finite size corrections and a careful scaling analysis[30,40,41] is required to establish long range order. Nevertheless, the growth in $S_{\rm AF}$ from $L = 8$ to $L = 16$ in Fig. 6(b) is certainly suggestive. The sharp onset at $t'/t \sim 0.6$ is similar to results reported in [21], as we shall discuss further below. $S_{\rm AF}$ appears to have a maximum at intermediate t'/t on the 8×8 lattice, an effect which is even more pronounced in the largest size, 16×16.

To understand this result better we show, in Fig.7, the

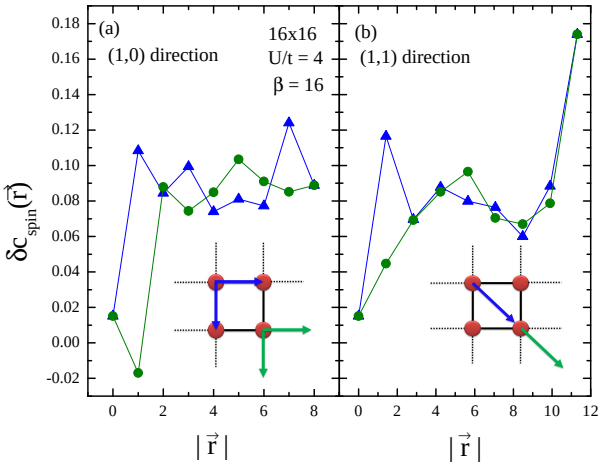

FIG. 7: (Color online) (a) Normalized difference of the spin correlation for the $t'/t = 0.8$ and the $t'/t = 1.0$ at a given position $\vec{r}$ along the equivalent NN lines ($(1,0)$ or $(0,1)$). The (green) circles are the correlations outward a plaquette while in the (blue) triangles are the same but the correlations start in a direction inside the plaquettes, as depicted in the inset. (b) the same as in (a) but for the $(1,1)$ direction, i.e., along the NNN links.

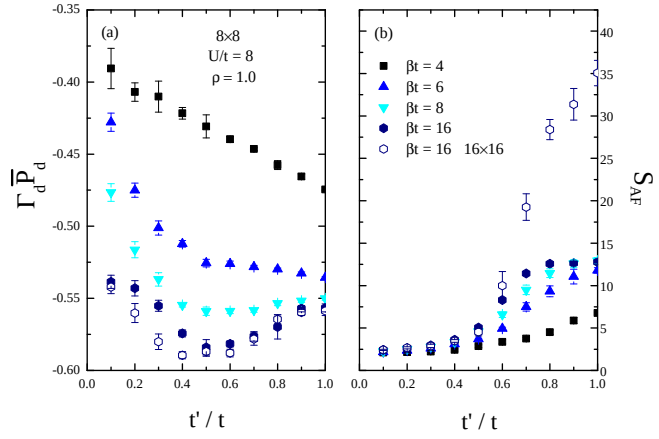

FIG. 8: (Color online) Similar to Fig. 6 except $U/t = 8$. The left panel shows the measure $\Gamma\bar{P}_d$ of the pairing instability as a function of inhomogeneity t'/t for different inverse temperatures, and the right panel is the antiferromagnetic structure factor. The lattice is half-filled $\rho = 1$.

normalized difference of the spin correlations,

$$\delta c_{\rm spin}(\vec{r}) = \frac{c_{\rm spin}^{t'=0.8}(\vec{r}) - c_{\rm spin}^{t'=1.0}(\vec{r})}{c_{\rm spin}^{t'=0.8}(\vec{r}) + c_{\rm spin}^{t'=1.0}(\vec{r})} \qquad (8)$$

Panel (a) has $\vec{r}$ along the (1,0) direction, and panel (b) along the (1,1) direction. With the exception of the correlation for spins which are first neighbors in different plaquettes, all values of $\vec{r}$ show an increase, $\delta c_{\rm spin} > 0$.

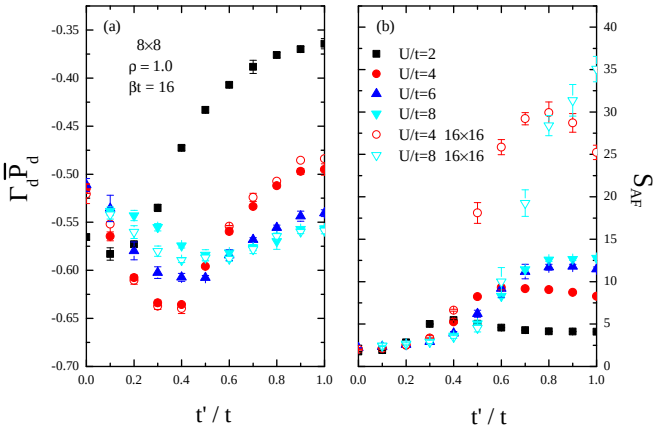

FIG. 9: (Color online) The tendency to (a) superconductivity $\Gamma\bar{P}_d$ and (b) antiferromagnetic structure factor S_{AF} as functions of inhomogeneity t'/t at fixed low temperature $\beta t = 16$ and filling $\rho = 1$ for different U/t.

What this tells us is that the enhancement in $S_{\rm AF}$ comes from an increase in the real-space spin correlations for all separations, and is not simply from an enhancement at short (or long) distances. The fact that $\delta c_{\rm spin}(\vec{r} = 0)$ is small further informs us that the effect is not just due to a trivial change in the local moment.

We conclude this section by showing half-filled results for different interaction strength U/t. In Fig. 8(left), the evolution with t'/t of the product of the d-wave superconducting vertex and the no-vertex susceptibility, $\Gamma_d\bar{P}_d$, is given for $U/t = 8$ and several temperatures. As the temperature is lowered, a clear minimum in $\Gamma\bar{P}_d$ indicates an optimal inhomogeneity, at a larger t'/t than for $U/t = 4$.

In Fig. 8(right), the antiferromagnetic structure factor is given. As the temperature decreases, the antiferromagnetic structure factor becomes larger. Similar to the case of $U/t = 4$, S_{AF} has an onset at $t'/t \sim 0.6$.

Figure 9 shows $\Gamma_d\overline{P}_d$ and S_{AF} for four different U/t values at fixed inverse temperature $\beta t = 16$. In Fig. 9(a), an optimal inhomogeneity is present for all U/t, shifting systematically to larger t'/t as U/t increases. We note this trend is generally consistent with what is shown in Fig. 4 of Ref. [19], Fig. 2 of Ref. [20], and Figs. 2,5 of Ref. [21]. The maximum in $|\Gamma\bar{P}_d|$ is most evident at $U/t = 4$, for this fixed inverse temperature $\beta t = 16$. Comparison of S_{AF} data for 8×8 and 16×16 lattices shows that the structure factor is growing roughly proportional to the volume, as expected in an ordered Neél phase. The magnetic structure factor also increases with U/t as double occupancy is suppressed.

B. The doped lattice

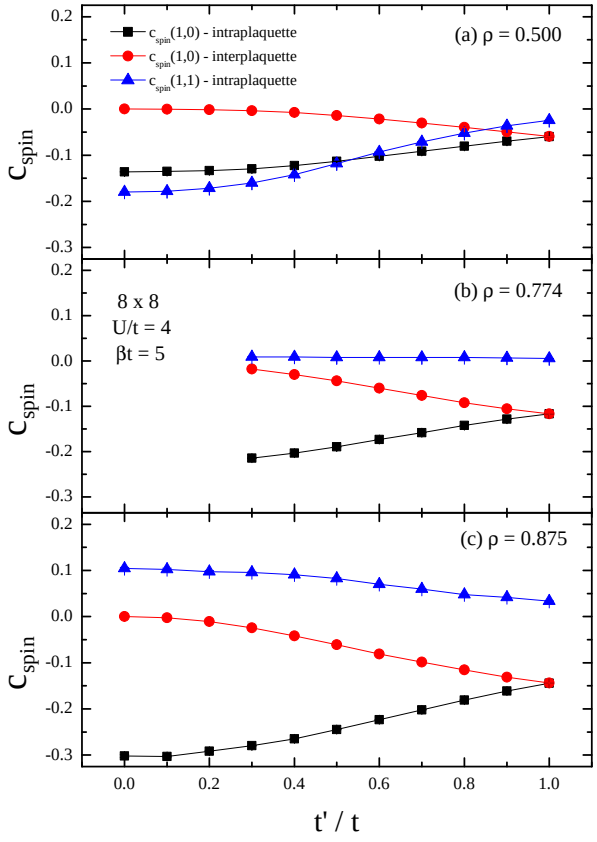

FIG. 10: (Color online) Spin correlations $c_{\rm spin}(1,0)$ along an intraplaquette (t) bond and along an interplaquette (t') bond. Also shown are next-near neighbor values inside a plaquette. The lattice size is 8×8, inverse temperature $\beta t = 5$ and interaction strength $U/t = 4$.

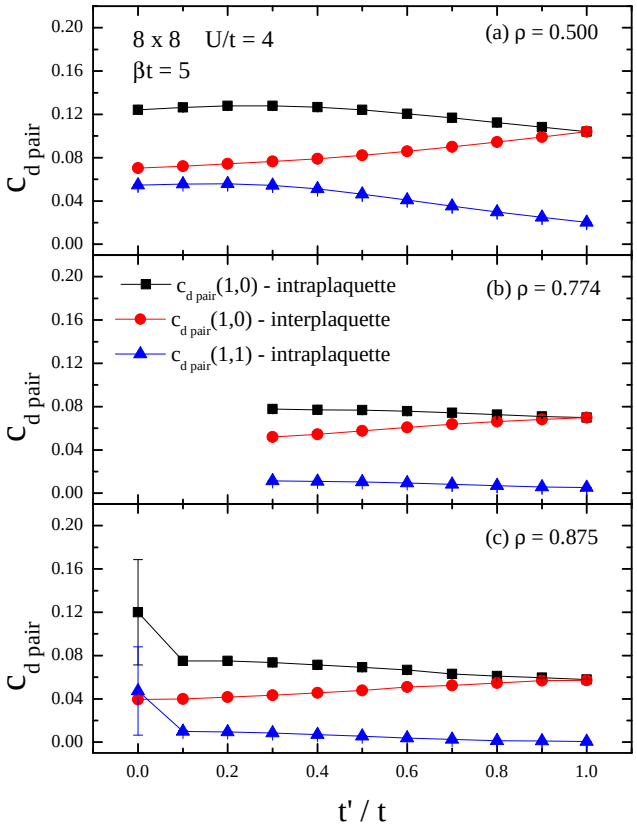

FIG. 11: (Color online) Near-neighbor and next-near neighbor d-wave pairing correlations as a function of t'/t. The lattice size is 8×8, inverse temperature $\beta t = 5$ and interaction strength $U/t = 4$.

After this brief synopsis of results at $\rho = 1$, we turn to the case when the filling is incommensurate, the situation of most interest to understanding cuprate superconductivity.

Fig. 10 shows the same spin correlations as in Fig. 5(a), but for $\rho = 0.500$ (a), $\rho = 0.774$ (b) and $\rho = 0.875$ (c). The NN spin correlations exhibit the expected evolution with density- they are largest at $\rho = 1.000$ (Fig. 5(a)), and decrease as we move away from half-filling. Similar to what happens at half-filling, the NNN spin correlation inside a plaquette is positive for $\rho = 0.875$, again as expected for antiferromagnetism, but decreases with growing t'. With decreasing density the behavior for this quantity changes: for $\rho = 0.774$, $c_{spin}(1,1)$ is essentially zero for all t'/t. For $\rho = 0.500$, however, it is *negative* and increases in magnitude as the connection between the plaquettes is reduced. This later result can be understood when we recall that at this density the system has two fermions in every plaquette on average. The configuration which minimizes the kinetic energy and the local repulsive interaction is a singlet state with spins residing on NNN neighbors. In this case the NNN correlation becomes negative. This effect is enhanced as t'/t is smaller.

Figure 11 shows short-range d-wave pair correlations for the same densities as Fig. 10. Contrary to what is observed for spin correlations, NN and NNN pairing correlations do not decrease with doping.

Having described the short range, real space correlations, we now turn to more sensitive magnetic and pairing structure factors and susceptibilities. The latter especially has an enhanced signal since it is sensitive to the build-up of correlations in the imaginary time direction. The magnetic structure factor dependence on t'/t and q_x, q_y for three different dopings on an 8×8 lattice at inverse temperature $\beta t = 5$ is shown in Fig. 12. Near half-filling ($\rho = 0.875, 0.774$) $S(q_x, q_y)$ is peaked at (π, π), indicating the dominance of antiferromagnetic correlations. At $\rho = 0.875$ the AF peak substantially increases as $t' \to t$, with a concomitant reduction in S at other momenta. Presumably these effects would become

larger at lower T. However, $\beta t \approx 5$ is the limit accessible to DQMC owing to the sign problem. For lower densities, $S(q_x, q_y)$ is rather insensitive to t'.

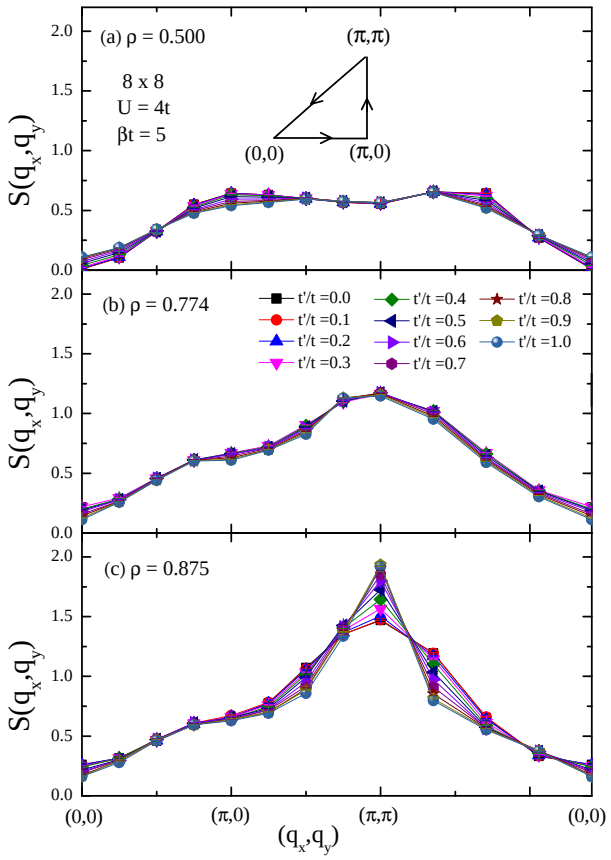

FIG. 12: (Color online) The equal time structure factor $S(q_x, q_y)$ is shown as a function of momentum as one traverses the Brillouin zone triangle shown in the panel (a) inset. Panels (a), (b) and (c) correspond to the dopings $\rho = 0.5, 0.774$, and 0.875 respectively. For each density, S is given for eleven different t'/t. The lattice size is 8×8, $U/t = 4$, and inverse temperature $\beta t = 5$.

There is a substantial difference in scale of the antiferromagnetic structure factor: $S_{\rm AF} = S(\pi, \pi) \sim 1$ in the doped lattice, whereas at half-filling, $S_{\rm AF} \sim 10$ (Fig. 6). This arises both from the rapid suppression of antiferromagnetic order with doping in the square lattice Hubbard model[30,31], and also because of the lower temperatures that can be reached at $\rho = 1$ ($\beta t \sim 10-16$) compared to $\rho \neq 1$ ($\beta t \sim 5$). Despite the absence of long range order in the doped model, the short range spin correlations do grow as T is lowered.

At $\rho = 0.875$ the overall evolution with t'/t of the antiferromagnetic structure factor $S(\pi, \pi)$ in Fig. 12 is consistent with that found in [21]. That is, $S(\pi, \pi)$ increases monotonically with t'/t and is maximal at $t'/t = 1$. However, the two results appear to differ in the finer details. Specifically, the CORE study indicates that the staggered magnetic order parameter is roughly constant for $0 < t'/t < 0.5$, and then increases rather abruptly at $t'/t \approx 0.6$. This is mirrored in an increase in the number of magnons, a phenomenon to which the appearance of a maximum in the pair binding energy is attributed. In contrast, our DQMC data appear to indicate a more immediate rise in $S(\pi, \pi)$ as t' grows from zero. A possible origin of the difference is that our work is at finite temperature, whereas the CORE study is in the ground state. Indeed, at half-filling it is known that $S(\pi, \pi)$ does not reach its low T values until $T/t \lesssim 0.08$, temperatures which are not accessible when the system is doped, due to the sign problem. That finite temperature is a likely explanation of the difference and is substantiated by examining the $\rho = 1$ data in Fig. 6. Interestingly, the rapid rise in $S_{\rm AF}$ occurs at the same $t'/t \sim 0.6$ obtained from CORE. Note that in [21] the number of holes is $N_h = 2, 4$ on a 6×6 cluster, corresponding to $\rho = 0.945, 0.890$. The latter value is comparable to that of Fig. 12(c).

Figure 13 extends the pairing results of Fig. 6(a) to the doped case. Although the sign problem currently prevents simulations at low T, all densities shown exhibit a maximum in $|\Gamma_d \overline{P}_d|$ away from the uniform limit $t'/t = 1$. For $\rho = 0.774$ and $\rho = 0.875$, the sign is fairly small for $\beta t = 5$ and small t'/t (see Fig. 2). We have thus done a very large number of runs (up to 100 runs with 50000 sweeps each), to decrease the error bars and push the limits of the QMC method. For $\rho = 0.5$, where the sign is higher, we were able to reach $\beta t = 7$ (open symbols). Similar to what is seen in Fig. 6(a), for $\rho = 1$, the signal for optimal inhomogeneity indeed increases as T is lowered. It is reasonable to assume that the same trend will hold for $\rho = 0.774$ and $\rho = 0.875$.

Almost all of the work presented in this paper is for $U/t = 4$. The sign problem in DQMC becomes dramatically worse as U/t increases. In order to study the U/t evolution and still reach reasonably low temperatures, we can reduce the density to $\rho = 0.5$ which restores the sign even though $U/t \gtrsim 4$. Even so, it is not possible for us to assess accurately claims[20–22] that $U/t \sim 8$ is optimal for pairing.

The choice $\rho = 0.5$ does however improve the average sign enough to see the t'/t evolution of d-wave pairing, which we established to have an optimal inhomogeneity at half-filling. Fig. 14 (a) shows $\Gamma_d \overline{P}_d$ versus T/t for different t'/t. As at $\rho = 1$, there is evidence for an optimal inhomogeneity: in the uniform case $\Gamma_d \overline{P}_d$ versus T/t is almost temperature independent and is also small, $|\Gamma_d \overline{P}_d| \lesssim 0.01$. As inhomogeneity is turned on to $t'/t \sim 0.5$, $|\Gamma_d \overline{P}_d|$ increases by almost an order of magnitude (although it is still far from the $\Gamma_d \overline{P}_d = -1$ criterion for a transition). Further increase of the inhomogeneity to $t'/t < 0.5$ decreases $|\Gamma_d \overline{P}_d|$. The same optimum $t'/t \sim 0.5$ can be seen for $\rho = 0.774$, as shown in Fig. 14(b).

Early in DQMC studies of the homogeneous square lattice it was established that d-wave pairing is the

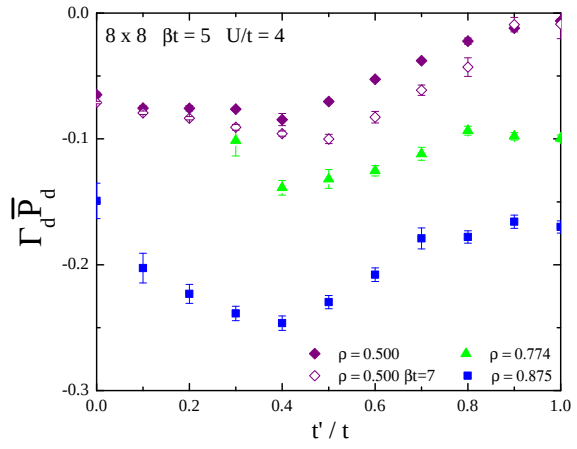

FIG. 13: (Color online) Dependence of the pairing vertex on t'/t away from half filling. All densities appear to show a maximum of $|\Gamma_d \overline{P}_d|$ at intermediate t'/t. The lattice size is 8 × 8, $U/t = 4$ and $\beta t = 5$. Also included for comparison the $\beta t = 7$ in the $\rho = 0.500$ case.

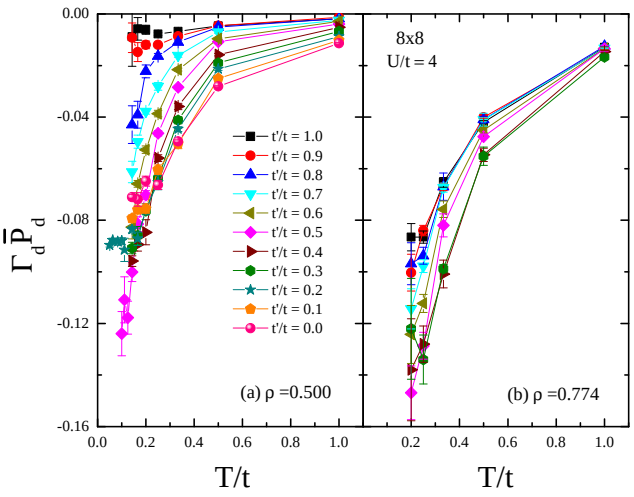

FIG. 14: (Color online) The evolution of $\Gamma_d \overline{P}_d$ with T/t for $\rho = 0.500$ (a) and $\rho = 0.774$ (b). The plots emphasize the existence of an optimal degree of inhomogeneity. Here the lattice size is 8 × 8 and $U/t = 4$.

dominant superconducting instability. This conclusion is not altered by $t' \neq t$. Fig. 15 shows the same quantities as Fig. 13 for s and *extended* s (s^*) symmetry channels. The correlations are obtained in a similar fashion as in the d-wave case but the associated phases in Eq. 5 are positive. For the s symmetry the pairs are created and destroyed locally $\left(\Delta^\dagger_{s\,\vec{r}} = c^\dagger_{\vec{r}\uparrow} c^\dagger_{\vec{r}\downarrow}\right)$, whereas in the extended one they all enter with the same phase sign $\left(\Delta^\dagger_{s^*\,\vec{r}} = c^\dagger_{\vec{r}\uparrow}(c^\dagger_{\vec{r}+\hat{x}\downarrow} + c^\dagger_{\vec{r}+\hat{y}\downarrow} + c^\dagger_{\vec{r}-\hat{x}\downarrow} + c^\dagger_{\vec{r}-\hat{y}\downarrow})\right)$. While s-wave symmetry produces only repulsive interactions, some parameters in the s^*-wave case exhibit attraction. Nonetheless it is smaller in magnitude than d-wave symmetry.

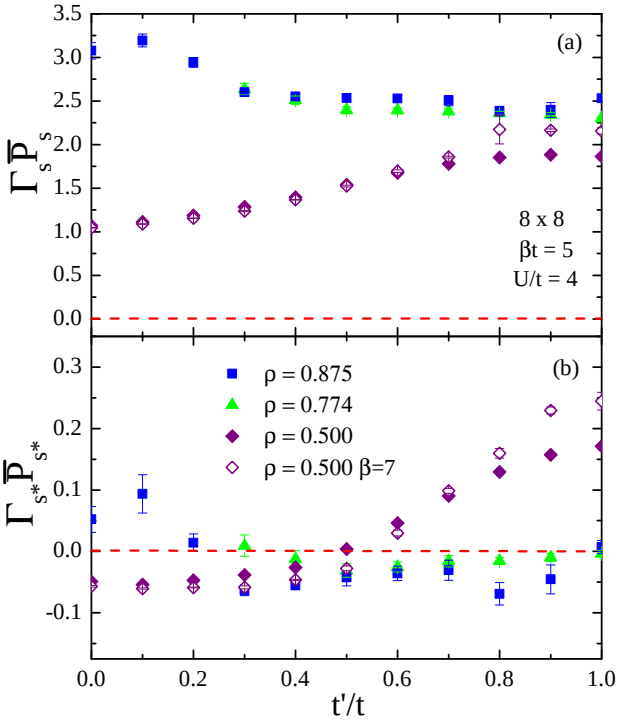

FIG. 15: (Color online) Same as Fig. 13 but now comparing the interaction vertex times the uncorrelated susceptibility for two other symmetry channels: s in (a) and s^* in (b). While in the former all densities result in a repulsion between the pairs for the whole range of t'/t studied, in the latter depending on the specific parameters the pairing turns attractive but is substantially smaller in magnitude in comparison to the d-wave symmetry channel.

IV. CHECKERBOARD HUBBARD MODEL

The nature of pairing in models with other sorts of inhomogeneities, e.g. built of two site dimers rather than four site clusters,[18] modulated by different site potentials[43] or consisting of lines of different chemical potentials, alternating between half-filled antiferromagnetic stripes and doped stripes has also been explored.[44] In this section we examine the effects on pairing of an inhomogeneity pattern in which the local energies on a regular pattern of sites is raised by an amount V_0. That is, we add a term $H' = V_0 \sum_{l\in\mathcal{A},\sigma} n_{l\sigma}$ to the Hubbard Hamiltonian Eq. 2 with $t' = t$. The collection $\mathcal{A}$ consists of a fraction f of the lattice sites.

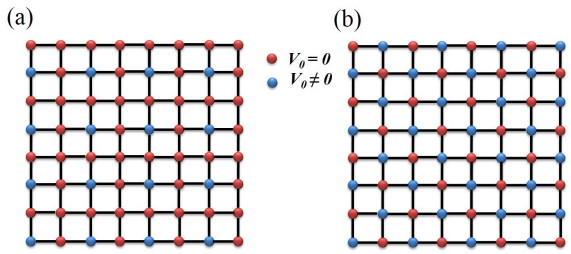

FIG. 16: (Color online) Checkerboard geometry, in which a fraction f of the sites, displayed in a checkerboard pattern, has on site energy raised by $V_0 \neq 0$. Panel (a) shows the $f = 1/4$ lattice and and (b) the $f = 1/2$ one, for 8×8 systems.

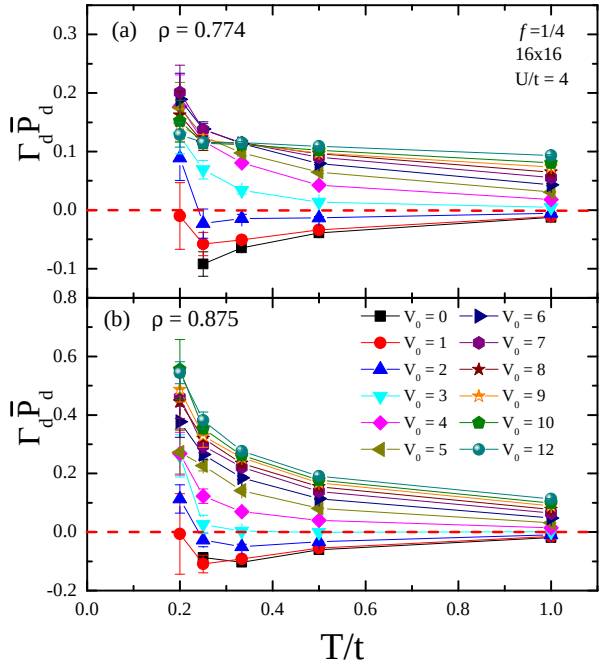

FIG. 17: (Color online) Product of interaction vertex Γ_d and uncorrelated susceptibility $\overline{P}_d$ for a Hubbard model with an alternating pattern of site energies. (See Fig. 16(a).) The vertex is weakly attractive for the homogeneous case, $V_0 = 0$, but becomes repulsive for $V_0 \gtrsim 1$. Here the lattice size is 16×16, filling $\rho = 0.774$ in (a) and $\rho = 0.875$ in (b), and interaction strength $U/t = 4$.

This geometry is illustrated in Fig. 16, for $f = 1/4$ (a) and $f = 1/2$ (b), the two cases analyzed here.

One motivation for considering this particular pattern with $f = 1/4$ is that in the limit $V_0 \to \infty$ the lattice maps onto the 'three band' Hamiltonian sometimes used to model the CuO_2 plane of the cuprate superconductors (with, however, the choice of equal copper d and oxygen p energies.) The red sites without any blue neighbors are like the Cu atoms, while the red sites with two blue

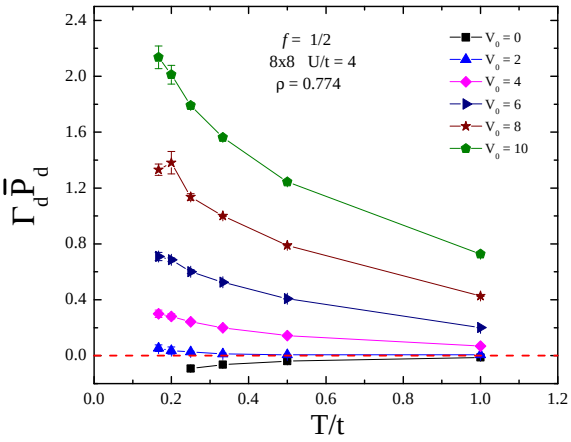

FIG. 18: (Color online) Same as Fig. 17, but for $f = 1/2$ and an 8×8 lattice. The qualitative behavior is similar to the $f = 1/4$ case: the site inhomogeneity drives the interaction vertex repulsive.

neighbors represent the O sites which link the Cu. Thus this model makes partial contact with earlier studies of binding on CuO_2 clusters in the limit $\epsilon_{pd} = 0$.[5–7] Another point of contact of this model is to other inhomogeneity patterns which share an $f = 1/4$ proportion of sites with raised on-site energy, for example [44] in which a pattern of stripes was shown to enhance d-wave pairing away from half-filling.

Results for this site-energy inhomogeneous geometry ($f = 1/4$) are shown in Fig. 17(a). In stark contrast to the plaquette model and to the *striped* V_0 model,[44] $\Gamma_d \overline{P}_d$ becomes positive when V_0 is turned on: the d-wave pairing vertex is made repulsive. As with the plaquette Hamiltonian of the previous sections, we are interested in how the dependence of pairing on inhomogeneity is affected by the density. To this end we show, in Fig. 17(b), the same quantity but with $\rho = 0.875$. This data is consistent with the previous density, and we conclude that this form of site energy inhomogeneity competes destructively with superconductivity.

Finally, we consider a pattern of inhomogeneity with $f = 1/2$. (see Fig. 16(b).) Fig. 18. demonstrates the effect of V_0 is monotonic and again inimical to superconductivity.

V. THE SIGN PROBLEM

We return here briefly to the sign problem which is the fundamental limitation to using DQMC to study lattice fermion Hamiltonians[38]. In generic situations (that is, in the absence of particle-hole or some other symmetry which makes the sign positive) the fermion sign $\langle \mathcal{S} \rangle$ is well-behaved down to some temperature

scale $T/t \sim \alpha$, where $\frac{1}{3} \lesssim \alpha \lesssim \frac{1}{5}$ depends, in the single band Hubbard model, on U and ρ. Below this temperature, $\langle \mathcal{S} \rangle$ decays exponentially with $\beta = 1/T$ so that simulations are feasible only in a very narrow range of temperatures below the point at which some of the fermion determinants begin to go negative. $\langle \mathcal{S} \rangle$ also decays exponentially with spatial volume V, but in practice the β dependence is usually more problematic. The behavior of $\langle \mathcal{S} \rangle$ with ρ and spatial geometry is also affected by 'shell effects',[45] so that the sign can remain close to unity for fillings for which multiple k points have the same non-interacting energy ϵ_k.

The plaquette Hubbard Hamiltonian offers a window into this V dependence, since it must be rigorously true at $t'/t = 0$ that $\langle \mathcal{S}(V = L \times L) \rangle = \langle \mathcal{S}(V = 2 \times 2) \rangle^{(L/2)^2}$. It is interesting, then, to understand how the coupling of independent plaquettes with $t'/t \neq 0$ modifies this manifestly exponential decay. We show results in Fig. 19. When $t'/t = 0$ (top panel) the average sign (symbols) precisely follows the prediction (dashed lines) based on the sign of an elemental 2×2 cluster. However, when the clusters are coupled, $t'/t = 0.6$ (bottom panel), the average sign is increased. While the improvement in the behavior of $\langle \mathcal{S} \rangle$ is not sufficient to allow ground state properties to be obtained, it is nevertheless intriguing, and non-trivial, that the entanglement of the clusters by hopping t' here reduces the sign problem: The coefficient γ of the exponential decay $\langle \mathcal{S} \rangle \propto e^{-\gamma V}$ changes from $\gamma \sim 0.056$, at $t'/t = 0.0$, to $\gamma \sim 0.014$, at $t'/t = 0.6$.

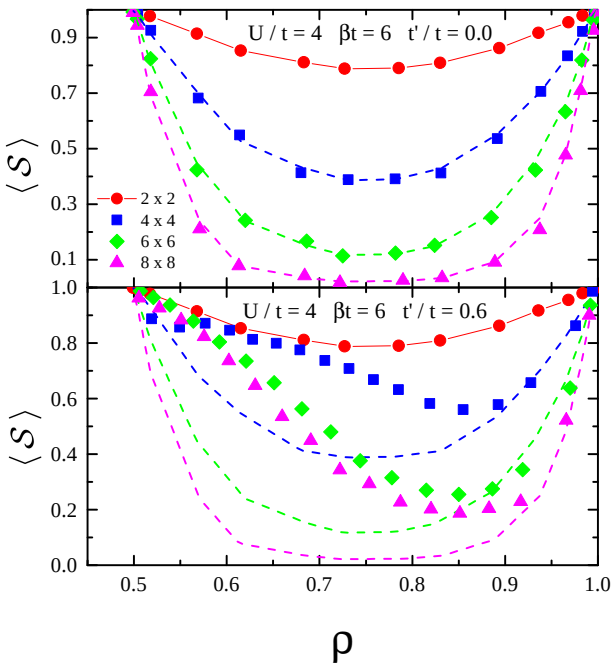

FIG. 19: (Color online) Top panel: Average sign $\langle \mathcal{S} \rangle$ as a function of filling ρ for $t = 1, U/t = 4, \beta t = 6$ and different system sizes. Interplaquette hopping $t'/t = 0$ so that system is composed of $(L/2)^2$ independent 2×2 clusters. Dashed lines are the prediction for the average sign obtained by taking the sign for a 2×2 lattice (i.e. a single plaquette) raised to the $(L/2)^2$ power. Bottom panel: Same except interplaquette hopping $t'/t = 0.6$. The fact that $\langle \mathcal{S} \rangle \sim 1$ for $\rho \sim 0.5$ is a 'shell effect'. (See text.)

VI. CONCLUSIONS

Study of the effect of inhomogeneities on superconductivity has been a focus of much computational effort on the Hubbard and $t - J$ models over the last decade. One branch of effort has explored models where inhomogeneity is included in the Hamiltonian itself. Other work concerns the question of inhomogeneity which arises spontaneously in a translationally invariant Hamiltonian. The plaquette Hubbard model has been a natural candidate of interest since it seems to contain the nascent element, a substantial binding energy, in its building blocks.

We have shown here that DQMC indicates that a sensitive measurement of d-wave pairing yields an 'optimal degree of inhomogeneity'. That is $\Gamma \overline{P}_d$ is closer to -1 at $t'/t \sim 0.4$ when $U/t = 4$ than at $t'/t = 0$ or $t'/t = 1$. Larger U/t lead to larger optimal t'/t for the $2 \leq U/t \leq 8$ range studied. This result agrees qualitatively with some past numeric work (differing in the precise optimal t'/t), but is in disagreement with several of the most powerful computational methods available for these sorts of problems. When simulations are conducted directly on doped lattices, our work clearly shows the existence of an optimal inhomogeneity, which develops further as T is lowered. While the sign problem prevents us from going to very low temperatures, we can further infer what happens for small doping through our results at half-filling, where there is little limitation on the accessible temperature. Here, as White *et.al.* have emphasized[30] the pair correlation function $c_{d\,\mathrm{pair}}(\vec{r}, \tau) = \langle \Delta_{d\,\vec{r}_0+\vec{r}}(\tau)\, \Delta^{\dagger}_{d\,\vec{r}_0}(0) \rangle$ probes the insertion and propagation of a pair of fermions in the half-filled lattice, resulting in an effective doping $\delta = 2/L^2$. On an 8×8 lattice, for example, this corresponds to $\delta \sim 0.03$. Direct simulations of the doped system would, of course, be preferable, especially since this effective doping is system size dependent. Nevertheless, comparisons of data for different $t'/t, U/t$ and (large) βt on lattices of *fixed* size are possible. In this way, our low temperature, half-filled results speak to the issue of the role of inhomogeneity. Simulations of an alternative 'checkerboard Hubbard model' show that the attractive d-wave vertex is not generic. A different pattern of spatial inhomogeneity produced a repulsive vertex for most parameter regimes of this second Hamiltonian.

We have also exploited the ability to decouple the model spatially to obtain data on the sign problem as independent ($t'/t = 0$) spatial clusters are coupled. We

find that the average sign is increased by finite t'/t.

We conclude this paper with a few remarks concerning the results from different numerical methods. Our DQMC results are most consistent with the exact diagonalization[20], DMRG[22], and CORE[21] treatments, indicating the existence of an optimal degree of inhomogeneity. As is well known, what makes the problem of strong correlation so challenging is the competition between different possible ordered (or disordered) states at low temperature which are close in energy. Even small approximations in analytic and numeric treatments can tip the balance in these near-degeneracies. DQMC treats the correlated electron problem exactly on lattices of finite size. Here, we are exploring a superconducting mechanism which explicitly attributes pairing to a spatially local attraction, as opposed to the exchange of lattice vibrations or spin waves. In such a situation it is plausible that finite size effects, while still present, might be less strong.

Acknowledgements: This work was supported by the National Key Basic Research Program of China, Grant No. 2013CB328702, by DOE DE-FG52-09NA29464, and by the Office of the President of the University of California. Support from CNPq and FAPERJ (TP and RM) is gratefully acknowledged.

[1] D.J. Scalapino and S.A. Trugman, Philos. Mag. B **74**, 607 (1996).
[2] J.A. Riera and A.P. Young, Phys. Rev. B **39**, 9697 (1989).
[3] E. Dagotto, A. Moreo, R.L. Sugar, and D. Toussaint, Phys. Rev. B **41**, 811 (1990).
[4] R.M. Fye, M.J. Martins, and R.T. Scalettar, Phys. Rev. B **42**, 6809 (1990).
[5] J.E. Hirsch, S. Tang, E. Loh, and D.J. Scalapino, Phys. Rev. Lett. **60**, 1668 (1988).
[6] C.A. Balseiro, A.G. Rojo, E.R. Gagliano, and B. Alascio, Phys. Rev. B **38**, 9315 (1988).
[7] J.E. Hirsch, E. Loh, and D.J. Scalapino, and S. Tang, Phys. Rev. B **39**, 243 (1989).
[8] J. Callaway, D.P. Chen, D.G. Kanhere, and Q. Li, Phys. Rev. B **42**, 465 (1990).
[9] E. Kaxiras and E. Manousakis, Phys. Rev. B **38**, 866 (1988).
[10] J. Bonca, P. Prelovsek, and I. Sega, Phys. Rev. B **39**, 7074 (1989).
[11] Y. Hasegawa and D. Poilblanc, Phys. Rev. B **40**, 9035 (1989).
[12] H. Yao, W-F. Tsai, and S.A. Kivelson, Phys. Rev. B **76**, 161104(R) (2007).
[13] H. Yao and S.A. Kivelson, Phys. Rev. Lett. **105**, 166402 (2010).
[14] P.M. Smith and M.P. Kennett, Phys. Rev. B **88**, 214518 (2013).
[15] E. Arrigoni, E. Fradkin, and S.A. Kivelson, Phys. Rev. B **69**, 214519 (2004).
[16] I. Martin, D. Podolsky, and S.A. Kivelson, Phys. Rev. B **72**, 060502(R) (2005).
[17] S.A. Kivelson and E. Fradkin, in *Handbook of High-Temperature Superconductivity*, edited by J.R. Schrieffer and J.S. Brooks (Springer, New York, 2007).
[18] W.F. Tsai and S.A. Kivelson, Phys. Rev. B **73**, 214510 (2006).
[19] R.M. Fye, D.J. Scalapino, and R.T. Scalettar, Phys. Rev. **B46**, 8667 (1992).
[20] W.-F. Tsai, H. Yao, A. Lauchli, and S. A. Kivelson, Phys. Rev. B **77**, 214502 (2008).
[21] S. Baruch and D. Orgad, Phys. Rev. B **82**, 134537 (2010).
[22] G. Karakonstantakis, E. Berg, S.R. White, and S.A. Kivelson, Phys. Rev. B **83**, 054508 (2011).
[23] D.G.S.P. Doluweera, A. Macridin, T. A. Maier, M. Jarrell, and T. Pruschke, Phys. Rev. B **78**, 020504(R) (2008).
[24] T. A. Maier, M. Jarrell, and D. J. Scalapino, Phys. Rev. B **74**, 094513 (2006).
[25] T.A. Maier, M. Jarrell, and D.J. Scalapino, Phys. Rev. B **75**, 134519 (2007).
[26] T.A. Maier, A. Macridin, M. Jarrell, and D.J. Scalapino, Phys. Rev. B **76**, 144516 (2007).
[27] S. Chakraborty, D. Sénéchal, and A.-M.S. Tremblay, Phys. Rev. B **84**, 054545 (2011).
[28] It is worth noting that there is a considerable literature on another model sometimes also referred to as the "checkerboard Hubbard Hamiltonian" (or "2D pyrochlore" Hamiltonian).[32–37] In this model, hopping is present along the diagonal of alternating plaquettes of the square lattice Hubbard Hamiltonian. One key question is whether a spin liquid phase in which there is no symmetry breaking emerges due to the frustration, or whether the ground state retains some sort of translation-invariance-breaking or exotic pairing order. The model considered in [13] contains elements both of a Hamiltonian built up of linked plaquettes and the frustrating effects of diagonal hopping.
[29] R. Blankenbecler, D.J. Scalapino, and R.L. Sugar, Phys. Rev. D **24**, 2278 (1981).
[30] S.R. White, D.J. Scalapino, R.L. Sugar, E.Y. Loh, Jr., J.E. Gubernatis, and R.T. Scalettar, Phys. Rev. B **40**, 506 (1989).
[31] J.E. Hirsch, Phys. Rev. B **31**, 4403 (1985).
[32] T. Yoshioka, A. Koga, and N. Kawakami, Phys. Rev. B **78**, 165113 (2008).
[33] F. Trousselet, D. Poilblanc, and R. Moessner, Phys. Rev. B **78**,195101 (2008).
[34] D. Poilblanc, K. Penc, and N. Shannon, Phys. Rev. B **75** 220503(R) (2007).
[35] H.X. Huang, Y.Q. Li, J.Y. Gan, Y. Chen, and F.C. Zhang, Phys. Rev. B **75**, 184523 (2007).
[36] M. Indergand, C. Honerkamp, A. Läuchli, D. Poilblanc, and M. Sigrist, Phys. Rev. B **75**, 045105 (2007).
[37] M. Raczkowski and D. Poilblanc, Phys. Rev. Lett. **103**, 027001 (2009).
[38] E.Y. Loh, J.E. Gubernatis, R.T. Scalettar, S.R. White, D.J. Scalapino, and R.L. Sugar, Phys. Rev. B **41**, 9301 (1990).
[39] J.E. Hirsch and S. Tang, Phys. Rev. Lett. **62**, 591 (1989).
[40] C.N. Varney, C.R. Lee, Z.J. Bai, S. Chiesa, M. Jarrell, and R. T. Scalettar, Phys. Rev. B **80**, 075116 (2009).
[41] D. A. Huse, Phys. Rev. B **37**, 2380 (1988).

[42] S.R. White, D.J. Scalapino, R.L. Sugar, N.E. Bickers, and R.T. Scalettar, Phys. Rev. B **39**, 839 (1989).
[43] S. Okamoto and T.A. Maier, Phys. Rev. B **81**, 214525 (2010).
[44] R. Mondaini, T. Ying, T. Paiva, and R.T. Scalettar, Phys. Rev. B **86**, 184506 (2012).
[45] R. Mondaini, K. Bouadim, T. Paiva, and R. R. dos Santos, Phys. Rev. B **85**, 125127 (2012).